

# Blind source separation-based tracking of ARFI-induced displacements for improved automatic delineation of carotid plaque components in humans, *in vivo*

Gabriela Torres

Joint Department of Biomedical Engineering  
University of North Carolina and North  
Carolina State University  
Chapel Hill, NC, USA

Tomasz J. Czernuszewicz

Joint Department of Biomedical Engineering  
University of North Carolina and North  
Carolina State University  
Chapel Hill, NC, USA

Caterina M. Gallippi

Joint Department of Biomedical Engineering  
University of North Carolina and North  
Carolina State University  
Chapel Hill, NC, USA

**Abstract**— Atherosclerotic plaque rupture potential is conferred by plaque composition and structure. We have previously shown in humans *in vivo* that carotid plaque components can be automatically delineated by a support vector machine (SVM) classifier considering normalized cross-correlation (NCC)-derived measures of ARFI-induced displacement. We now extend our prior work by hypothesizing that classification is improved by using displacements derived using blind source separation (BSS). In 20 carotid plaques imaged *in vivo* in patients undergoing carotid endarterectomy (CEA) were imaged prior to extraction, and specimens were harvested after CEA for histological processing. ARFI displacement profiles were calculated from each of the first five principal components of the RF data and used as inputs to the SVM classifier. The classifier was evaluated by 5-fold cross-validation, with the histological samples acting as gold standards. From the output SVM likelihood matrices, ROC curves were calculated for separating collagen from calcium and lipid-rich necrotic core from intraplaque hemorrhage. For all examined plaques, inputting displacement profiles derived from the first four eigenvectors to the SVM classifier increased sensitivity and specificity over using NCC-derived displacement profiles. These results suggest that using BSS-derived displacement profiles as inputs to the SVM classifier improves discrimination of carotid plaque components that are correlated to vulnerability for rupture.

**Keywords**—ARFI imaging, carotid plaque, blind source separation.

## I. INTRODUCTION

Atherosclerosis is the most common cause of cardiovascular diseases and of death worldwide [1]. Unfortunately, atherosclerotic conditions usually stay silent until very late stages when plaque rupture can cause ischemic events. The asymptomatic nature of atherosclerosis makes it challenging to prevent, identify, monitor and treat. However, appropriate clinical management is especially critical for atherosclerotic plaques in the carotid artery, as it prevents stroke while simultaneously minimizing risks associated with carotid endarterectomy (CEA) surgeries. It is estimated that as many as 13 out of 14 symptomatic patients with 50-69% stenosis and 21 out of 22 asymptomatic patients with 70-99% stenosis undergo

CEA unnecessarily [2]. Improved identification of vulnerable carotid plaque is critically needed to differentiate patients at low risk of embolic stroke from those in crucial need of CEA to prevent it.

The term *vulnerable plaque* is defined as a plaque with high rupture risk and likelihood for generating an ischemic event [2]. These plaques vary in location, size, and structure between patient to patient. Rather than size or degree of stenosis, their relative risk is determined by their structure and composition [3]. Recent studies have shown histologically that plaque composition is a better biomarker than degree of stenosis for assessing vulnerability to rupture [5]. More specifically, histopathological post-mortem studies [2-4] have defined the hallmarks of vulnerable plaques to include one or more of the following components: thin fibrous caps, large lipid-rich necrotic cores, increased vasa-vasorum neovascularization, inflammation, and presence of intra-plaque hemorrhage.

Currently, the clinical standard for carotid plaque evaluation is duplex ultrasound. However, this technique does not delineate plaque structure and composition. As an alternative, Acoustic Radiation Force Impulse (ARFI) imaging has been demonstrated in animal models and in humans, with validation by spatially matched histology [10, 11]. Further, the sensitivity and specificity of ARFI imaging for delineating collagen (COL), calcium (CAL), lipid rich necrotic core (LRNC), and intraplaque hemorrhage (IPH) has been demonstrated for human carotid plaque, *in vivo* [13]. In a statistical reader study with histological validation, ARFI-induced peak displacement (PD) was evaluated as a metric for tissue stiffness, with high displacing regions associated with soft (LRNC and IPH) and low displacing regions associated with stiff (COL and CAL) plaque features. Although ARFI PD achieved high sensitivity and specificity for distinguishing grouped soft (LRNC & IPH) from grouped stiff (COL & CAL) components, PD had low sensitivity and specificity for discriminating between soft and between stiff elements. Alternative ARFI-derived parameters such as variance of acceleration (VoA) have been developed to improve separation of individual plaque components [16]. More recently, we have previously shown in humans *in vivo* that carotid plaque components can be automatically delineated by a support vector

machine (SVM) classifier considering normalized cross-correlation (NCC)-derived measures of ARFI-induced displacement [17]. In order to improve ARFI-based classification between carotid plaque components, we herein evaluate an alternative ARFI displacement tracking method based on Blind Source Separation (BSS). We hypothesize that SVM classification is improved by using blind source separation (BSS)-derived displacements as inputs. We test this hypothesis using ARFI data acquired in vivo in 20 carotid plaques from 25 patients undergoing carotid endarterectomy (CEA) and spatially matched histology evaluated by a trained pathologist.

## II. METHODS

### A. Clinical protocol

Patient data were acquired during a previous clinical study as described in [13]. A total of 25 patients undergoing clinically indicated CEA were recruited from UNC Hospitals. Inclusion criteria included asymptomatic carotid artery disease with >60% Doppler-indicated stenosis and unresponsive to medical management, or symptomatic carotid artery disease with a stenosis suspected to be the source of emboli. All procedures were institutional review board (IRB)-approved, and informed consent was given from each study participant.

A total of 20 carotid plaque samples were selected based on the following criteria: (1) spatially alignment with histology without fractures, and (2) mean ARFI image quality (as assessed by blinded readers  $\geq 2$ ) [13].

### B. ARFI imaging

A Siemens Acuson Antares imaging system (Siemens Medical Solutions USA, Inc., Ultrasound Division) equipped for research purposes was used for in vivo imaging with a VF7-3 linear array transducer. ARFI excitation pulses were 300-cycles at 4.21 MHz, and tracking pulses were 2-cycles at 6.15 MHz.

A registered sonographer acquired the imaging data before patient sedation, on the same day of surgery. Longitudinal B-mode and ARFI images of the plaque were acquired, using electrocardiogram (ECG) gating to trigger acquisition during diastole. Raw RF data were saved for off-line processing using MATLAB (Mathworks Inc., Natick, MA). The time interval between imaging and specimen extraction was approximately four hours. The plaque to be removed by CEA was identified from prior ultrasound imaging sessions archived in the patients' medical records and was typically the plaque with the greatest stenosis. Before completing the imaging session, the transducer

was rotated 90°, and transverse B-modes and CINE loops of the carotid bifurcation were obtained for alignment with histology.

### C. Blind source separation (BSS) displacement tracking

Using radio frequency data, ARFI-induced displacements were measured using normalized cross correlation (NCC) with a  $1.5\lambda$  (376- $\mu\text{m}$ ) kernel, two-stage interpolation, and linear motion filtering [14].

For BSS-based displacement tracking, the acquired radio frequency data was Hilbert transformed, then underwent principal component decomposition. The Fourier transform of the phase was calculated for the  $n$ th most energetic principal component (where  $n = 1,2,3,4,5$ ). Next, the phase velocity is computed from the frequency spectra, applied through translating axial kernels. Principal component analysis assumes that the source signals are orthogonal and Gaussian-distributed. Both BSS and NCC tracking were performed using a  $1.5 \lambda$  mm kernel.

### D. Plaque component classification

ARFI displacement profiles were calculated from each of the first five principal components of the RF data and used as inputs to a support vector machine (SVM) algorithm. Four output classes were defined as CAL, COL, LRNC, and IPH. The algorithm was trained by inputs corresponding to each independent class, previously validated by spatially-matched histology delineated by a pathologist. Parameter tuning was performed using Bayesian optimization. The classifier was evaluated by 5-fold cross-validation with histological gold-standard. From the output SVM likelihood matrices, ROC curves were calculated for separating COL from CAL, and LPNC from IPH. ROC results achieved using BSS-derived displacement profiles were compared those achieved using NCC-derived displacements. 2D class likelihood maps were calculated as the compounded likelihood per pixel assigned to an RGB value per class:

1. IPH = [255 0 0]
2. LRNC = [255 255 0]
3. COL = [0 255 255]
4. CAL = [0 0 255]

where colors between the above RGB values represent combined likelihoods of two classes.

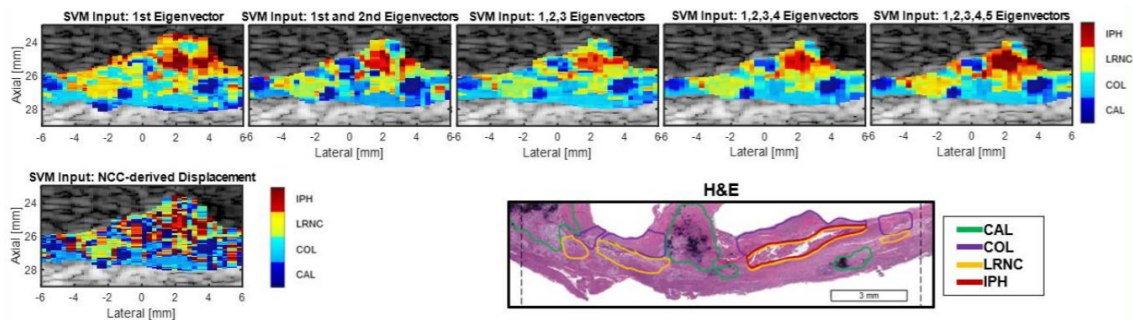


Fig. 1. SVM feature-likelihood images for example Type Va Plaque in 53 y/o female with different classification inputs, with matched histology.

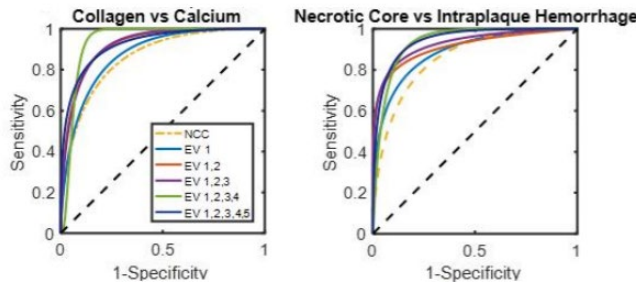


Fig. 2. Parametric receiver operating characteristic (ROC) curves for Eigenvector-based SVM classifiers for identifying collagen (COL) vs. calcium (CAL), and necrotic core (LRNC) vs. intraplaque hemorrhage (IPH).

### III. RESULTS AND DISCUSSION

Figure 1 shows SVM feature-likelihood images derived from the analyzed eigenvector combinations, and also when using the NCC-tracked displacements as input, for a type Va plaque with spatially matched histology.

TABLE I. PERFORMACE FOR EIGENVECTOR-BASED SVM CLASSIFIER FOR IDENTIFYING COLLAGEN (COL) VS CALCIUM (CAL), AND NECROTIC CORE (LRNC) VS INTRAPLAQUE HEMORRHAGE (IPH).

Eigenvector inputs for SVM Classifier	COL vs CAL		LRNC vs IPH	
	Sensitivity	Specificity	Sensitivity	Specificity
1	0.826	0.764	0.795	0.760
1, 2	0.870	0.820	0.839	0.838
1, 2, 3	0.878	0.814	0.854	0.853
1, 2, 3, 4	0.970	0.853	0.917	0.828
1, 2, 3, 4, 5	0.844	0.844	0.886	0.857
NCC-derived disp.	0.653	0.712	0.659	0.622

Figure 2 shows that, for all examined plaques, using displacement profiles derived from the first four eigenvectors as SVM inputs increased sensitivity and specificity over using NCC-derived displacement profiles. Specifically, Table 1 shows that for differentiating COL vs CAL, using the first four eigenvector as inputs provided the maximum improvement of 39.1% and 18% in sensitivity and specificity, respectively, in comparison to NCC. Similarly, for differentiating LRNC vs IPH, these improved 32.7%, and 28.4% in sensitivity and specificity, respectively.

### IV. CONCLUSION

Displacement profiles derived from the first four eigenvectors as inputs to the SVM classifier increased sensitivity and specificity over using NCC-derived displacement profiles. These results suggest that using BSS-derived displacement profiles as inputs to the SVM classifier improves the discrimination of carotid plaque components that are correlated to vulnerability for rupture.

### ACKNOWLEDGMENT

The authors thank Siemens Healthcare, Ultrasound Division for in-kind support. This work was supported by UNC Glaxo Foundation Fellowship and NIH grants R01HL092944, R01NS074057, R01DK107740, K02HL105659, and T32HL069768. The authors also appreciate the contribution K. A. Yokoyama for help with manuscript editing.

### REFERENCES

- [1] E. J. Benjamin, et al., "Heart disease and stroke statistics-2017 Update: a report from the American Heart Association," *Circulation*, vol. 135, no. 10 pp. e146-e603, 2017.
- [2] P. R. Moreno, "Vulnerable plaque: definition, diagnosis, and treatment," *Cardiol. Clin.*, vol. 28, no. 1, pp. 1-30, 2010.
- [3] P. K. Shah, "Mechanisms of plaque vulnerability and rupture," *J. Am. Coll. Cardiol.*, vol. 41, pp. 15S-22S, 2003.
- [4] H. C. Stary, "Natural history and histological classification of atherosclerotic lesions: an update," *Arterioscler. Thromb. Vasc. Biol.*, vol. 20, pp. 1177-8, 2000.
- [5] A. Gupta, et al., "Carotid plaque MRI and stroke risk: a systematic review and meta-analysis," *Stroke*, vol. 44, pp. 3071-3077, 2013.
- [6] J. J. Dahl, et al., "Acoustic radiation force impulse imaging for noninvasive characterization of carotid artery atherosclerotic plaques: a feasibility study," *Ultrasound Med. Biol.*, vol. 35, pp. 707-716, 2009.
- [7] R. H. Behler, et al., "ARFI imaging for noninvasive material characterization of atherosclerosis. Part II: toward in vivo characterization," *Ultrasound Med. Biol.*, vol. 35, pp. 278-295, 2009.
- [8] J. D. Allen, et al., "The development and potential of acoustic radiation force impulse (ARFI) imaging for carotid artery plaque characterization," *J. Vasc. Med.*, vol. 16, pp. 302-311, 2011.
- [9] T. J. Czernuszewicz, and C. M. Gallippi, "On the Feasibility of Quantifying Fibrous Cap Thickness with Acoustic Radiation Force Impulse (ARFI) Ultrasound," *IEEE Trans. Ultrason. Ferroelectr. Freq. Control*, vol. 63, pp. 1262-1275, 2016.
- [10] R. H. Behler, et al., "Acoustic radiation force beam sequence performance for detection and material characterization of atherosclerotic plaques: preclinical, ex vivo results," *IEEE Trans. Ultrason. Ferroelectr. Freq. Control*, vol. 60, pp. 2471-2487, 2013.
- [11] T. J. Czernuszewicz, et al., "Non-invasive in vivo characterization of human carotid plaques with acoustic radiation force impulse ultrasound: comparison with histology after endarterectomy," *Ultrasound Med. Biol.*, vol. 41, pp. 685-697, 2015.
- [12] S. D. Williamson, et al., "On the sensitivity of wall stresses in diseased arteries to variable material properties," *J. Biomech. Eng.*, vol. 125, no. 1, pp. 147-155, 2003.
- [13] T. J. Czernuszewicz, et al., "Performance of Acoustic Radiation Force Impulse Ultrasound Imaging for Carotid Plaque Characterization with Histological Validation," *Journal Vasc. Surg.*, in press, 2017.
- [14] K. Nightingale, M. S. Soo, R. Nightingale, G. E. Trahey, "Acoustic radiation force impulse imaging: in vivo demonstration of clinical feasibility," *Ultrasound Med. Biol.*, vol. 28, pp. 227-235, 2002.
- [15] G. F. Pinton, J. J. Dahl, and G. E. Trahey, "Rapid tracking of small displacements with ultrasound," *IEEE Trans. Ultrason. Ferroelectr. Freq. Control*, vol. 53, no. 6, pp. 1103-1117, 2006.
- [16] G. Torres, T. J. Czernuszewicz, J. W. Homeister, M. C. Caughey, B. Y. Huang, E. R. Lee, C. A. Zamora, M. A. Farber, W. A. Marston, D. Y. Huang, T. C. Nichols, "Delineation of Human Carotid Plaque Features In Vivo by Exploiting Displacement Variance," *IEEE transactions on ultrasonics, ferroelectrics, and frequency control*. 2019;66(3):481-92.
- [17] G. Torres, T. J. Czernuszewicz, J. W. Homeister, M. A. Farber, C. M. Gallippi, "A Machine Learning Approach to Delineating Carotid Atherosclerotic Plaque Structure and Composition by ARFI Ultrasound, In Vivo," *2018 IEEE International Ultrasonics Symposium (IUS) 2018 Oct 22 (pp. 1-4)*.